Colloid Polym Sci (2006) 284: 688–693
DOI 10.1007/s00396-005-1454-7

SHORT COMMUNICATION

Kiyoshi Shibata
Takayuki Yamamoto
Masahiko Kurita
Hiroshi Kimura
Akira Tsuchida
Tsuneo Okubo

Photon trapping by the internal Bragg reflection of colloidal crystals

Received: 25 July 2005
Accepted: 3 December 2005
Published online: 27 January 2006

K. Shibata · T. Yamamoto · M. Kurita · H. Kimura · A. Tsuchida (✉)
Department of Applied Chemistry,
Faculty of Engineering,
Gifu University,
1-1 Yanagido,
Gifu 501-1193, Japan
e-mail: tsuchida@apchem.gifu-u.ac.jp
Tel.: +81-58-2932624
Fax: +81-58-2301893

T. Okubo
Institute for Colloidal Organization,
3-1-112 Hatoyama, Uji, Kyoto 611-0012,
Japan and Cooperative Research Center,
Yamagata University,
4-3-16 Jonan,
Yonezawa, Yamagata 992-8510, Japan

Abstract Fluorescence light emitted from photoexcited rhodamine 6G (R6G) doped in colloidal crystals of exhaustively deionized colloidal silica suspension is partially trapped within a crystal cage. This photon trapping is caused by Bragg reflection in crystal lattices. The photon trapping efficiencies were quantitatively examined as a function of the thickness of measurement cell. The efficiency increased from about 40 to 60% as the cell thickness increased from 1 to 10 mm for an R6G concentration of 5×10^{-6} mol/L. This result is attributed to an increase in the number of crystal layers perpendicular to the observation direction; these are formed in the cell with a large optical path length. On the other hand, the trapping efficiencies were constant irrespective of the angle between the incident and observed light of the cylindrical cells. The constant efficiencies are attributed to the fact that the heterogeneous crystal layers around the inner cell wall have the same thickness.

Keywords Colloidal crystal · Rhodamine 6G · Bragg reflection · Fluorescence spectra · Photon trapping

Introduction

When a suspension of monodispersed colloidal spheres is exhaustively deionized in polar solvents such as water, a crystal-like structure is formed [1–4]. This colloidal crystal is formed due to the extended electrical double layers around the spheres and Brownian motion of the spheres. Because the lattice spacing of the colloidal crystal matches with the wavelength range of visible light, the crystal shows bright iridescent colors when irradiated with white light. More than a decade ago, Okubo [5] succeeded in fabricating very large single crystals, 2–8 mm in size. Recently, the authors have reported the optical properties of colloidal crystals including electro-optic [6–8] and rheo-optic [9, 10] effects.

The possibility of a photonic band gap (PBG) was identified recently [11]; since then, many researchers have studied photonic crystals, which are two- or three-dimensional periodic structures in which the refractive index changes with the length in the order of the optical wavelength, to use them as practical optical materials [11–14]. Photonic crystals hold the promise of important technological applications, e.g., optical switching and computing. In the search for effective PBG crystals, colloidal crystals are interested in fabricating the photonic crystals comprising a three-dimensional periodic array of micrometer or nanometer particles. Bogomolov et al. [15] observed a dip in the fluorescence spectra of rhodamine 6G (R6G) molecules embedded in an artificial opal. The opal crystal was filled with various liquids to change the relative refractive index of silica. The position of the dip varied depending on the relative refractive index of silica with respect to the liquids, and the photon trapping effect was reported. Koenderink et al. [16] reported that in the case of photonic crystals made of inverse opals in titania doped with R6G, the fluorescence intensity was attenuated independent of the observation angle.

In this study, the photon trapping efficiencies are examined for colloidal crystals of silica spheres in deionized water. By the use of R6G-containing suspension of colloidal silica spheres, the photon trapping efficiencies were quantitatively measured as a function of the position in the measurement cell and the thickness of cells, i.e., crystal layers of the colloidal crystals. Furthermore, the angle between the excitation light and the observed fluorescence was changed from 90° to 180° using cylindrical cells, and the variation in the photon trapping efficiency was examined.

Experimental

Materials

An aqueous suspension of colloidal silica spheres (CS82) was donated by Catalyst & Chemical Ind. Co., Ltd. (Tokyo, Japan). The sphere diameter was determined to be 103±13.2 nm (mean diameter±standard deviation) by an electron microscopy. The suspension was treated in a mixed bed of cation- and anion-exchange resins (AG501-X8(D), Bio-Rad Lab., Hercules, CA, USA) for more than 8 years to eliminate ionic impurities as completely as possible. The purest grade of cationic dye of R6G (Aldrich, Milwaukee, WI, USA; dye content 99%) was used without further purification. The maximum R6G dye concentration in the aqueous CS82 suspension was limited to 1×10^{-5} mol/L to avoid aggregation, concentration quenching, and apparent fluorescence quenching due to reabsorption of the dye; further, because of the limited concentration, the critical concentration of the melting of the crystals was prevented from increasing. When the R6G solution was mixed with the colloidal suspension, the ion-exchange resins were removed because the resins adsorb the R6G molecules. Highly pure water obtained from the Milli-Q water system (Milli-RO Plus and Milli-Q Plus, Millipore Ltd., Bedford, MA, USA) was used. Precautions were taken to avoid ionic contamination in the sample preparation.

The volume fraction (ϕ) of the silica spheres in the suspension was adjusted to 0.0427 to match the Bragg peak wavelength of the crystals with the fluorescence band of R6G (λ_{max}=550 nm). The intersphere distance of colloidal crystals can be calculated using Eqs. (1) and (2) [17, 18].

$$l_0 = 0.904 d_0 \phi^{-1/3} \quad (1)$$

$$l_{obs} = 0.6124 \lambda_p n^{-1} \quad (2)$$

where l_0 denotes the distance calculated from the diameter (d_0) and volume fraction (ϕ) of the colloidal silica spheres, and l_{obs} denotes the distance determined from the Bragg peak wavelength (λ_p) and refractive index of the suspension (n). In this study, the value of n is approximated to that of water (1.333). In the case of CS82 crystals with ϕ=0.0427, the Bragg peak was determined to be at λ_p=575 nm by measuring the reflection spectrum. The values of l_0 and l_{obs} are calculated to be 266 and 264 nm, respectively. Both l_0 and l_{obs} agreed within the experimental error.

Measurements

Quartz rectangular cells [inner size=1, 2, 5, or 10 mm (optical path lengths)×10 mm (width)×48 mm (height)] and cylindrical cells (inner diameter=4.2 or 10 mm) were used in the measurements. For the reflection spectra measurements, a light beam from a halogen light source (PHL-50, Sigma Koki, Saitama, Japan) was introduced perpendicular to each observation cell wall through a Y-type optical fiber; the incident light beam was then focused on the inner cell wall (diameter <1.5 mm). The reflection spectra were recorded on a photonic multichannel analyzer (PMA-50, Hamamatsu Photonics, Hamamatsu, Japan). Absorption spectra were obtained using a spectrophotometer (U-3500, Hitachi, Tokyo, Japan) by employing rectangular cells.

Fluorescence spectra were measured using a spectrofluorophotometer (U-4500, Hitachi). Three types of experiments, shown schematically in Fig. 1, were performed using different slit layouts. Figure 1a shows the measurements of the photon trapping efficiencies at different positions inside the cell. The fluorescence spectra were observed perpendicular (θ=90°) to the direction of the excitation light using a rectangular cell (inner size=10×10 mm). Two slits (slit width=1 mm) were placed: one on the excitation light side and the other on the fluorescence observation side. The positions of the slits were changed along the excitation light axis or the fluorescence observation axis as shown in the left- and right-hand sides of Fig. 1a, respectively. In the former case, the slit on the excitation light side was fixed at the center, whereas that on the fluorescence observation side was shifted along the excitation light axis; that is, the fluorescence spectra were measured as a function of the transmitted length of the excitation light in the colloidal suspension. On the other hand, in the latter case, the slit on the fluorescence observation side was fixed at the center, whereas that on the excitation light side was shifted along the fluorescence observation axis; that is, the fluorescence spectra were measured as a function of the transmitted length of the fluorescence light in the colloidal suspension. Figure 1b shows the measurements of the photon trapping efficiencies for different cell thicknesses. The fluorescence spectra were obtained at the opposite side (θ=180°) of the excitation light using rectangular cells (optical path length=1, 2, 5, or 10 mm). Two slits (slit width=3 mm) were placed on the excitation light and fluorescence observation sides to eliminate light scattering. Further, a sharp cut filter (SC48, Fuji Photo Film, Tokyo, Japan) was set on the fluorescence observation side to prevent contamination

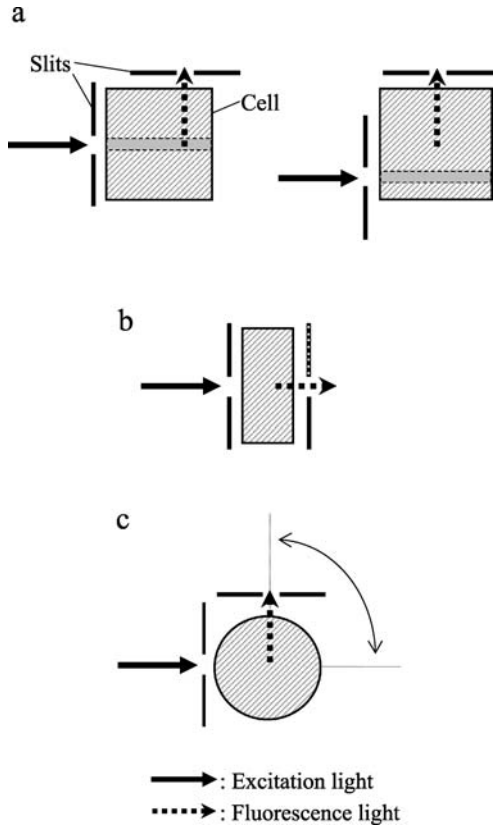

Fig. 1 Slit layouts in the measurements of fluorescence spectra

of the excitation light. Figure 1c shows the measurements of the photon trapping efficiencies at different angles between the excitation light and fluorescence observation directions. The excitation light was introduced in the cylindrical cells (inside diameter=4.2 or 10 mm) via an optical fiber, and the fluorescence light emitted from the sample was transmitted to a detector via another optical fiber. Two slits (slit width=1 mm) were mounted on the cell edges of the excitation and observation optical fibers. The fluorescence spectra were observed by rotating the observation optical fiber from θ=90° to 180° with respect to the excitation optical fiber.

For measurements using colloidal crystals, the colloidal suspensions were first stirred and then allowed to stand for more than 30 min (at 25±1°C in an air-conditioned room) to attain as high a degree of crystallinity as possible.

Results and discussion

Figure 2 shows typical examples of the absorption and fluorescence [excitation wavelength (λ_{ex})=480 nm] spectra of R6G. The spectra are good mirror images of each other; this is because of the negligible reabsorption of the dye at a low concentration of 1×10^{-6} mol/L. For the maximum dye concentration of 1×10^{-5} mol/L used in this study, the reabsorption was slightly recognized for the blue-side edge of the fluorescence band. However, it was negligible at λ_p=575 nm where the photon trapping efficiencies were estimated.

Figure 3a and Fig. 3b show the reflection and fluorescence spectra of CS82 suspension doped with R6G (5×10^{-5} mol/L), respectively. The spectra were obtained 30 min after mixing when the crystallinity of CS82 spheres in the cell was sufficiently high. Interestingly, a depletion in the R6G fluorescence was observed in Fig. 3b at the Bragg reflection wavelength (λ_p=575 nm), shown in Fig. 3a. This depletion is considered to be caused by the photon trapping due to the Bragg reflection when fluorescence light is emitted from the central region of the cell [19]. Figure 3c shows the fluorescence spectra for the same suspension measured immediately after the mixing. The peak intensities of the fluorescence spectra are normalized to unity. A comparison of Fig. 3c with Fig. 3b clearly indicates that the fluorescence depletion at 575 nm is caused by the existence of colloidal crystals in the cell. This process was completely reversible: the depletion disappeared after mixing the suspension and appeared after it settled. Figure 3d shows the fluorescence spectra of R6G in water without the CS82 spheres. The shape of the fluorescence spectra was almost the same as those measured in CS82 suspension, whereas a slight peak shift to the blue side was observed. This shift may be apparently caused by light scattering due to CS82 spheres at the blue side. In the CS82 suspension (ϕ=0.0427) doped with R6G (5×10^{-6} mol/L), about 64% of R6G molecules were found to be adsorbed on the CS82 colloidal particles (about 30 R6G dyes on single CS82 sphere) by examining the centrifuged supernatant of the suspension. Some R6G dyes may aggregate on the CS82 surface and cause a red shift of the spectrum.

The valley depth of the depletion, i.e., the photon trapping efficiency, is estimated from the fluorescence spectra by the method illustrated in Fig. 4. Two fluorescence spectra of R6G doped in CS82 suspension with crystals (30 min after mixing) and without crystals [NaCl

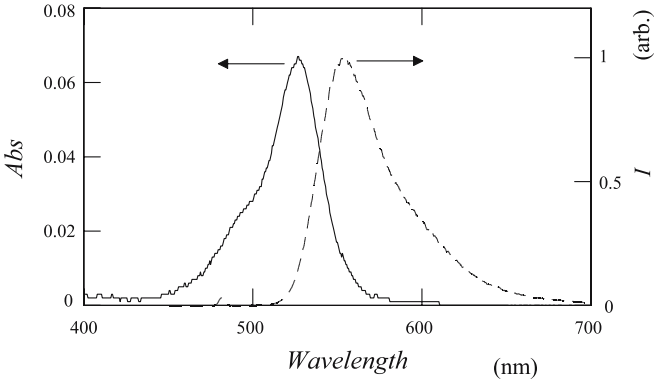

Fig. 2 Absorption (*solid line*) and fluorescence (*broken line*) spectra of rhodamine 6G (R6G; 1×10^{-6} mol/L) in water λ_{ex}=480 nm

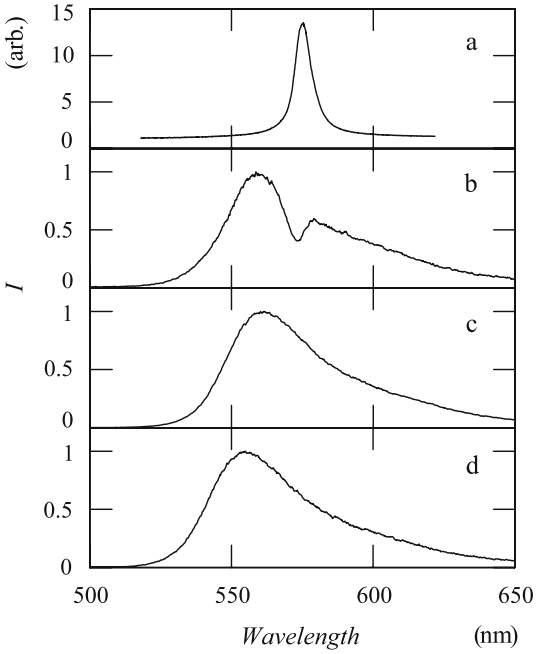

Fig. 3 Reflection (**a**) and fluorescence (**b**, **c**, **d**) spectra of R6G (5×10^{-6} mol/L) doped in CS82 (ϕ=0.0427) suspension. **a, b** Thirty minutes after mixing. **c** Immediately after mixing. **d** R6G in water without CS82 spheres

(5×10^{-5} mol/L) was added to melt the crystals] overlapped with each other at the red-side tail (about 600–700 nm). The difference between the fluorescence intensities (I) is divided by the fluorescence intensity (I') measured without crystals at the Bragg peak wavelength (λ_p=575 nm). This value of I/I' is the photon trapping efficiency; the greater the value of I/I', the higher is the trapping efficiency. In this comparison, the degree of adsorption of R6G dyes on CS82 spheres is inconsequential because the crystallization of these spheres scarcely affects the adsorption condition.

Figure 5 shows the I/I' values measured at different cell positions using the slit layouts shown in Fig. 1a. The center position of the slit is denoted by the value of l, which is the distance from the inner cell wall on the excitation light side or fluorescence observation side, along the excitation light axis or the fluorescence observation axis (left or right inset in Fig. 5), respectively. The value of l was changed from 2 to 8 mm in both cases. In Fig. 5, plots from a to b (denoted by circles) or from c to d (crosses) are the I/I' values obtained as a function of the transmittance length (l) of excitation or fluorescence light in the colloidal suspension, respectively. Clearly, in the former case, the I/I' values are approximately constant irrespective of l, whereas in the latter case, they increase with l. A reasonable interpretation of these results is that the fluorescence light at the Bragg peak wavelength emitted from the cell's interior is reflected by the crystal layers, thereby leading to attenuated fluorescence. A higher photon trapping efficiency is attained due to the larger number of crystal layers in the colloidal crystals.

The dependency of photon trapping efficiencies I/I' on the thickness of crystal layers was also investigated by changing the optical path length of rectangular cells with the alignment shown in Fig. 1b. Figure 6 shows the values of I/I' plotted against the cell thickness (d). The concentration of R6G was changed from 1×10^{-6} to 1×10^{-5} mol/L. At the low R6G concentration of 1×10^{-6} mol/L, the values of I/I' decreased with an increase in d. The value of I/I' increased and then saturated at a constant value for the intermediate R6G concentration of 5×10^{-6} mol/L. The I/I' value was the maximum at d=2 mm for high R6G concentration of 1×10^{-5} mol/L. These results can be explained by the following two reasons. First, the single crystal size of colloidal crystals increases due to a decrease in the nucleation rate [5, 20]. Exhaustive deionization of the suspension increases the nucleation rate; however, the competition between many simultaneous crystal growths decreases the discrete crystal size. In fact, while observing with the naked eye, larger crystals were observed for [R6G]=5×10^{-6} and

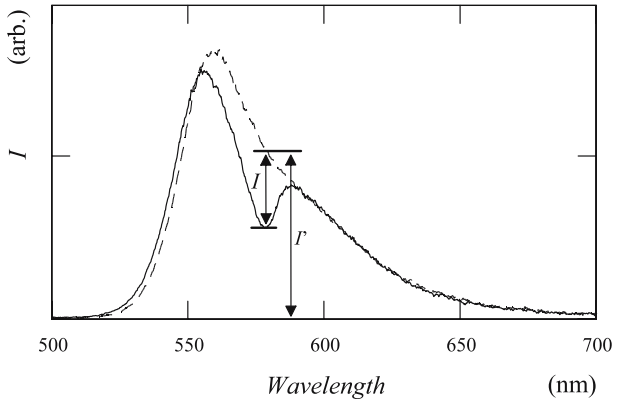

Fig. 4 Fluorescence spectra of R6G (5×10^{-6} mol/L) doped in CS82 (ϕ=0.0427) suspension. I: attenuated intensity, I': original intensity at the Bragg peak wavelength. *Solid curve*: without NaCl and 30 min after mixing, *broken curve*: with NaCl (5×10^{-5} mol/L)

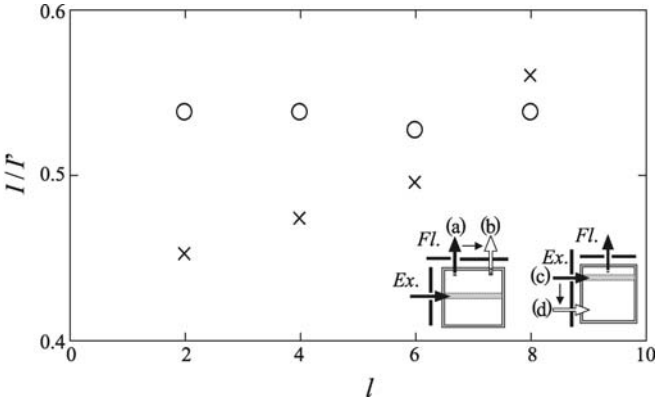

Fig. 5 Ratio of attenuated intensity (I) to original intensity (I') for R6G (5×10^{-6} mol/L) fluorescence doped in CS82 (ϕ=0.0427) suspension. The *circle and cross symbols* denote the changes of l from **a** to **b** along the excitation light axis and from **c** to **d** along the fluorescence light axis, respectively

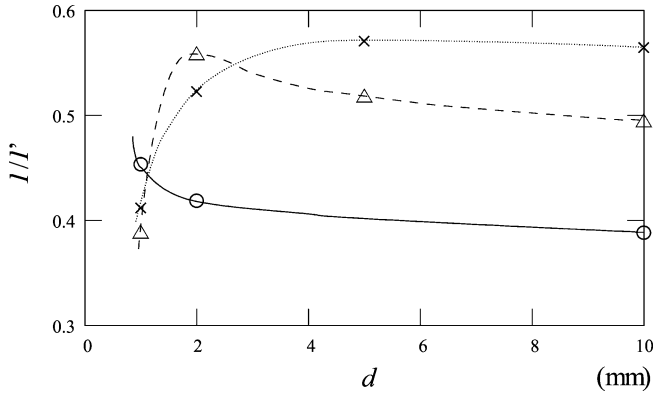

Fig. 6 Ratio of attenuated intensity (I) to original intensity (I') for R6G fluorescence doped in CS82 (ϕ=0.0427) suspension as a function of optical path length (d). ○: [R6G]=1×10^{-6} mol/L, ×: 5×10^{-6} mol/L, △ : 1×10^{-5} mol/L

1×10^{-5} mol/L as compared with 1×10^{-6} mol/L. It is considered that a large crystal size enhances the photon trapping efficiency because many crystal layers are aligned in the same direction. Second, the heterogeneous crystals grown from the cell wall are considered to lead to large I/I' values as compared with homogeneous crystals in the bulk phase of the suspension [5]. The crystal layers of the heterogeneous crystals are parallel to the cell wall, whereas those of the homogeneous crystals are at random angles to the observation direction. The cell with a small optical path length occupies a large fraction of the heterogeneous crystals.

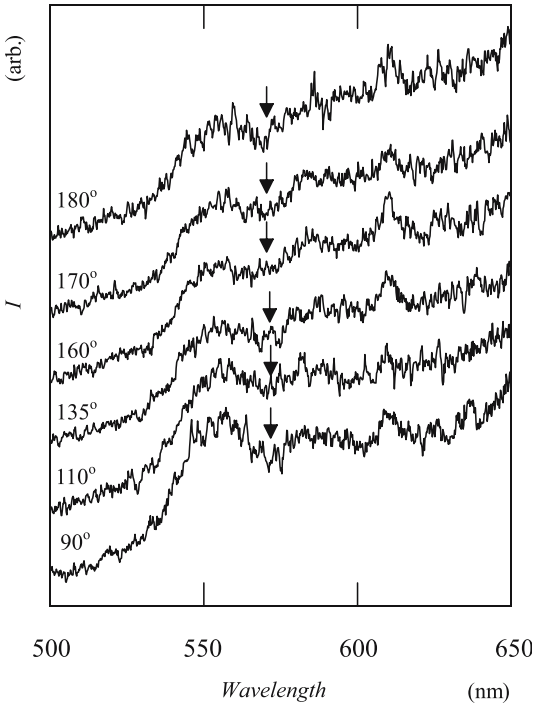

Fig. 7 Fluorescence spectra of R6G (5×10^{-6} mol/L) doped in CS82 (ϕ=0.0427) suspension measured at θ=90°, 110°, 135°, 160°, 170°, and 180° angles in a cylindrical cell (inner diameter=10 mm)

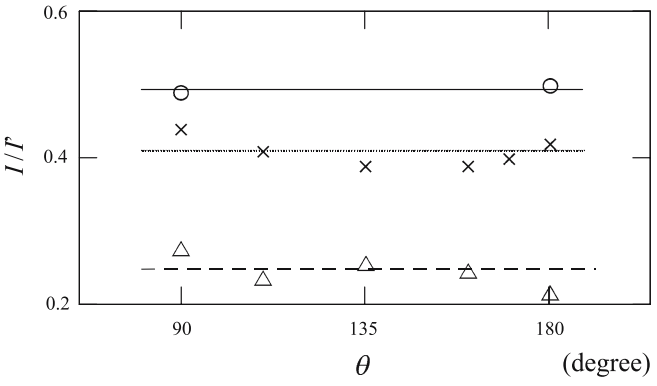

Fig. 8 Ratio of attenuated intensity (I) to original intensity (I') for R6G (5×10^{-6} mol/L) fluorescence doped in CS82 (ϕ=0.0427) suspension as a function of measurement angle (θ). ○: rectangular cell, ×: cylindrical cell (inner diameter=10 mm), △: cylindrical cell (inner diameter=4.2 mm)

The photon trapping efficiencies I/I' were measured as a function of the angle between the excitation light and fluorescence observation directions using cylindrical cells with the alignment shown in Fig. 1c. Figure 7 shows the fluorescence spectra of R6G (5×10^{-6} mol/L) in the colloidal suspension obtained using a 10-mm cylindrical cell. The measurement angles were changed from θ=90° (bottom of Fig. 7) to 180° (top). Depletions in the fluorescence bands are observed clearly at the Bragg wavelength of the crystals; these are indicated by arrows; however, the spectra are noisy due to the low efficiency of light transport of the two optical fibers used to guide both the excitation and fluorescence light. These depletions were observed using a 4.2-mm cylindrical cell. Figure 8 shows the I/I' values plotted against the angle θ. The I/I' values obtained using the rectangular cell (10×10 mm) at θ=90° and 180° are also shown. Although the experimental errors are not small, the I/I' values for each cell are approximately constant irrespective of θ. The average I/I' values are about 0.5, 0.4, and 0.25 for the rectangular cell, 10-mm cylindrical cell, and 4.2-mm cylindrical cell, respectively. The decrease in the photon trapping efficiency for the cell with a high wall curvature is attributed to the small fraction of the heterogeneous crystal layers aligned perpendicular to the observation direction. The higher efficiency of the photon trapping of colloidal crystals is attained by the larger crystal layers that are in good alignment perpendicular to the observation direction. With regard to the trapped photons, the fluorescence quantum yield (Φ) of R6G in water is about 0.9 [21], and 10% of the excited R6G is considered to be quenched by nonradiative deactivation in every reabsorption process.

Conclusions

The main conclusions from the present study are as follows. When a suspension of colloidal crystals is irradiated with an

external light source, a peak is observed in the reflection spectrum due to Bragg reflection. On the other hand, when light is emitted by photoexcited fluorescent dyes inside the suspension, a depletion is observed in the fluorescence spectrum. This depletion is caused by photon trapping inside the crystals due to Bragg reflection. The photon trapping efficiency increases with an increase in the number of crystal layers. Further, a good alignment of the crystal layers perpendicular to the observation direction is important for achieving a high photon trapping efficiency.

Acknowledgements Drs. M. Komatsu and M. Hirai of Catalyst & Chemical Ind. Co. (Tokyo, Japan) are thanked deeply for their providing the sample of the colloidal silica spheres. This research was partially supported by the Ministry of Education, Science, Sports and Culture, Grant-in-Aid for Scientific Research (B), 60183076, 2004.

References

1. Vanderhoff W, van de Hul W, Tausk RJM, Overbeek JThG (1970) In: Goldfinger G (ed) Clean surfaces: their preparation and characterization for interfacial studies. Marcel Dekker, New York
2. Pieranski P (1983) Contemp Phys 24:25
3. Ottewill RH (1985) Ber Bunsenges Phys Chem 89:281
4. Okubo T (1988) Acc Chem Res 21:281
5. Okubo T (1993) Prog Polym Sci 18:481
6. Okubo T, Tsuchida A (2002) Forma 17:141
7. Tsuchida A, Kuzawa M, Okubo T (2002) Colloids Surf 209:235
8. Tsuchida A, Shibata K, Okubo T (2003) Colloid Polym Sci 281:1104
9. Okubo T, Kimura H, Kawai T, Niimi H (2003) Langmuir 19:6014
10. Okubo T, Kimura H, Hatta T, Kawai T (2002) Phys Chem Chem Phys 4:2260
11. Yablonovitch E (1987) Phys Rev Lett 58:2059
12. Mekis A, Chen JC, Kurland I, Fan S, Villeneuve PR, Joannopoulos JD (1996) Phys Rev Lett 77:3787
13. Noda S, Yamamoto N, Kobayashi H, Okano M (1999) Appl Phys Lett 75:905
14. Kosaka H, Kawashima T, Tomita A, Notomi M, Tamamura T, Sato T, Kawakami S (1999) Appl Phys Lett 74:1370
15. Bogomolov VN, Gaponenko SV, Germanenko IN, Kapitonov AM, Petrov EP, Gaponenko NV, Prokofiev AV, Ponyavina AN, Silvanovich NI, Samoilovich SM (1997) Phys Rev E 55:7619
16. Koenderink AF, Bechger L, Lagendijk A, Vos WL (2003) Phys Status Solidi A 197:648
17. Okubo T (1986a) J Chem Soc Faraday Trans 82:3163
18. Okubo T (1986b) J Chem Soc Faraday Trans 82:3175
19. Megens M, Wijnhoven JEGJ, Lagendijk A, Vos WL (1999) J Opt Soc Am B 16:1403
20. Okubo T, Fujita H, Kiriyama K, Yamaoka H (1996) Colloid Polym Sci 274:73
21. Magde D, Wong R, Seybold PG (2002) Photochem Photobiol 75:327